AFRL-RW-EG-TR-2011-128

A COMPUTATIONAL EXAMINATION OF DETONATION PHYSICS AND BLAST CHEMISTRY

Christopher C. Buchanan

AFRL/RWPC
101 W. Eglin Blvd.
Eglin AFB, FL 32542-6810

August 2011

INTERIM REPORT

AIR FORCE RESEARCH LABORATORY
MUNITIONS DIRECTORATE

■ Air Force Materiel Command ■ United States Air Force ■ Eglin Air Force Base, FL 32542

NOTICE AND SIGNATURE PAGE

Using Government drawings, specifications, or other data included in this document for any purpose other than Government procurement does not in any obligate the U.S. Government. The fact that the Government formulated or supplied the drawings, specifications, or other data does not license the holder or any other person or corporation, or convey any rights or permission to manufacture, use, or sell any patented invention that may relate to them.

This report was cleared for public release by the 96th Air Base Wing, Public Affairs Office, and is available to the general public, including foreign nationals. Copies may be obtained from the Defense Technical Information Center (DTIC) < http://www.dtic.mil/dtic/index/html>.

AFRL-RW-EG-TR-2011-128 HAS BEEN REVIEWED AND IS APPROVED FOR PUBLICATION IN ACCORDANCE WITH ASSIGNED DISTRIBUTION STATEMENT.

FOR THE DIRECTOR:

Craig M. Ewing, DR-IV, PhD
Technical Adviser
Strategic Planning and Assessment Division

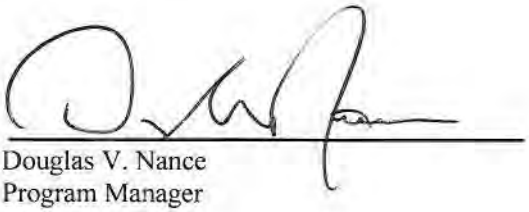

Douglas V. Nance
Program Manager

This report is published in the interest of scientific and technical information exchange, and its publication does not constitute the Government's approval or disapproval of its ideas or findings.

REPORT DOCUMENTATION PAGE

Form Approved
OMB No. 0704-0188

PLEASE DO NOT RETURN YOUR FORM TO THE ABOVE ADDRESS.

1. REPORT DATE *(DD-MM-YYYY)*	2. REPORT TYPE	3. DATES COVERED *(From - To)*
31-08-2011	INTERIM	29-05-2011 - 29-07-2011

4. TITLE AND SUBTITLE

A Computational Examination of Detonation Physics and Blast Chemistry

5a. CONTRACT NUMBER

N/A

5b. GRANT NUMBER

N/A

5c. PROGRAM ELEMENT NUMBER

62602F

6. AUTHOR(S)

Christopher C. Buchanan

5d. PROJECT NUMBER

2502

5e. TASK NUMBER

67

5f. WORK UNIT NUMBER

63

7. PERFORMING ORGANIZATION NAME(S) AND ADDRESS(ES)

AFRL/RWPC
101 W. Eglin Blvd.
Eglin AFB, FL 32542-6810

8. PERFORMING ORGANIZATION REPORT NUMBER

AFRL-RW-EG-TR-2011-128

9. SPONSORING/MONITORING AGENCY NAME(S) AND ADDRESS(ES)

AFRL/RWPC
101 W. Eglin Blvd.
Eglin AFB, FL 32542-6810

10. SPONSOR/MONITOR'S ACRONYM(S)

AFRL-RW-EG

11. SPONSOR/MONITOR'S REPORT NUMBER(S)

AFRL-RW-EG-TR-2011-128

12. DISTRIBUTION/AVAILABILITY STATEMENT

DISTRIBUTION A. Approved for public release, distribution unlimited. (96ABW-2011-0390)

13. SUPPLEMENTARY NOTES

NONE

14. ABSTRACT

This report makes preliminary steps in considering the detonation process for condensed explosives and the chemistry in the field of detonation products as linked physical entities. The desired end state of this research is improved control over explosive energy release. The report begins with a review of detonation physics with attendant algorithms for predicting detonation pressures. The second part of the report includes calculations of turbulent blast chemistry based upon an initial detonation solution for an HMX-based explosive. This chemistry includes a basic carbon soot model. Soot production is calculated over the first 27.5 microseconds of the blast event. Comparisons are shown between models of pure soot nucleation and nucleation with surface growth. Recommendations for further research are included.

15. SUBJECT TERMS

detonation, explosive, turbulence, soot, LES

16. SECURITY CLASSIFICATION OF:			17. LIMITATION OF ABSTRACT	18. NUMBER OF PAGES	19a. NAME OF RESPONSIBLE PERSON
a. REPORT	b. ABSTRACT	c. THIS PAGE			Douglas V. Nance
UNCLAS	UNCLAS	UNCLAS	UL	27	19b. TELEPHONE NUMBER *(Include area code)*

Reset

TABLE OF CONTENTS

LIST OF FIGURES

LIST OF FIGURES

1.0 INTRODUCTION

Detonation physics is a field with its roots in the investigations of combustion wave properties by Hugoniot (1887-1889), Chapman (1889) and others.[1] A solid understanding of the development and consequences of these and other fundamental studies is crucial to any research into the mechanics of detonation and into the subsequent blast. In the simplest sense, we can regard blast as an interaction of the detonating explosive with its surroundings, e.g., the air or neighbouring structures. The present work also constitutes a brief investigation into blast chemistry—the interaction of detonation products with the air and with themselves to form other products. The detonation/blast environment is highly complex due to the presence of multiple species and chemical processes with varying rates. A proper and more complete understanding of these dynamics may lead to ways of controlling blast effects. This is a topic of significant interest to the US Air Force. The present work begins with a discussion of basic detonation theory to orient the reader to our topic of interest. Moreover, we illustrate that conventional detonation theory treats energy release as a single lumped chemical parameter. Although we will begin to depart from this idea, it is essential to understand the ideal theory in that it provides a simple linkage between detonation chemistry and blast thermodynamics.

A computer program to illustrate this theory has been constructed for gaseous detonation products which may satisfy either of two equations of states. The first corresponds to the calorically-perfect gas (CPG) equation of state, and the second to the Jones-Wilkins-Lee (JWL) equation of state. The first is chosen because it is a simple, yet appropriate, introduction to solving fundamental detonation physics problems. The second is widely used and has been proven reliable when practical application is required, so incorporating it into the simple framework previously developed results in a comprehensive, powerful, and simple tool for predicting detonation conditions. This hydrodynamic analysis makes for a thorough evaluation of the essential physics governing the detonation problem lending immediately to practical application. Model validation exercises are performed using five well known explosive compounds. Program results are shown to correlate well with experiments.

As a second technical topic, we develop a subroutine to simulate chemical reactions in the post-detonation environment. This subroutine is employed by LESLIE3D, Large Eddy Simulation with LInear Eddy modeling in 3 Dimensions, a computer program developed by Suresh Menon at the Georgia Institute of Technology.[2] It simulates the time evolution of the shock wave, keeping up with such flow field parameters as pressure, temperature, and velocities while performing dynamic large eddy simulation. In this context, large eddy simulation (LES) is a family of techniques that divides the numerical estimation of properties into two parts. First, filtered governing equations are solved at scales larger than the mesh size. The solution at these "resolved" scales relies upon the numerical solution of the governing partial differential equations. Secondly, scales below the level of the grid cells require a modeling approach. In this case, our model of the subgrid stress tensor exploits self-similarity through a mathematical analogy with the Leonard stress. Most simulations with this level of complexity deal only with

the fluid products of detonation, but common explosives also produce soot, which is unique in that it is a solid product. It is hoped that further understanding of the formation of solid byproducts may provide greater insight into the mechanisms of explosive energy loss. In this study, soot particles are considered to be made entirely of carbon. Soot develops within the blast as a result of four primary stages: nucleation, surface growth, oxidation, and agglomeration.[3] We have already tested a nucleation model for soot, but observation has shown that young soot particles display very rapid mass growth in the presence of soot precursors like acetylene.[3] This fact motivates the present study. Here, the soot formation mechanism is enhanced by adding a second step to the reaction mechanism—surface growth due to the adsorption of acetylene on the surface of the particles. It takes into account the growing diameter size, its effect on the surface growth reaction rate, and the effect that aging throughout the flame reduces the reactivity of the soot particles.

Results of this investigation are compared, in the case of detonation conditions, to well established detonation criterion for multiple explosive compounds, and in the case of the soot formation and kinetics along a shock wave, to an earlier study which excludes soot surface growth. Primarily, it is hoped that future studies will allow new explosives to function with increased efficiency, particularly by maximizing energy release per unit explosive mass. With this motivation in mind, adding the third step in our soot model, oxidation, to the simulation may increase our understanding of the chemistry required to tailor the loading of oxidizer versus explosive compound in the material. In time, advanced simulation techniques like those described in part below may provide insight for improving the manufacturing and loading of metalized explosive components such as aluminum particles.

2.0 DETONATION PHYSICS

2.1 Technical Approach

For a one-dimensional steady flow combustion wave, treating the products and reactants as compressible fluids and fixing the coordinate system to the detonation wave front, the basic conservation equations of mass, momentum, and energy are given by

$$\rho_0 u_0 = \rho_1 u_1 \tag{1}$$

$$p_0 + \rho_0 u_0^2 = p_1 + \rho_1 u_1^2 \tag{2}$$

$$h_0 + \frac{u_0^2}{2} = h_1 + \frac{u_1^2}{2} \tag{3}$$

where $i = 0{,}1$ will hereafter represent the initial and final states, respectively; ρ_i is the density of the mixture; u_i is the velocity of the mixture with respect to the combustion wave; p_i is the pressure of the mixture, and h_i is the enthalpy per unit mass of the mixture. These three equations are sufficient to define the Rayleigh Line [3],

$$\frac{p_1 - p_0}{v_1 - v_0} = -\rho_0^2 u_0^2 = -\rho_1^2 u_1^2 \tag{4}$$

where $v_i = 1/\rho_i$ is the specific volume. Equations (1) through (4) may also be used to define the Hugoniot Equation [1], a relationship completely independent of the equation of state, i.e.,

$$h_1 - h_0 - q = \frac{1}{2}(p_1 - p_0)(v_0 + v_1) \tag{5}$$

where $q = h_{f_0}^o - h_{f_1}^o$ is the difference between the enthalpies of formation of reactants and products. When q is positive, (5) is referred to as the detonation Hugoniot. When $q = 0$, this equation relates thermodynamic states in unreacted material and is denoted the shock Hugoniot. As an example, the shock pressure for a calorically perfect gas may be written as

$$p_1 = \left\{ \frac{\left[\left(\frac{\gamma_0 + 1}{\gamma_0 - 1} \right) - \frac{v_1}{v_0} + \frac{2q}{p_0} \right]}{\left[\left(\frac{\gamma_1 + 1}{\gamma_1 - 1} \right) \frac{v_1}{v_0} - 1 \right]} \right\} p_0 \tag{6}$$

where γ_i is given by

$$\gamma_i = \frac{\mathrm{C_{p,}}_i}{\mathrm{C_{p,}}_i - \mathrm{R}} \tag{7}$$

$\mathrm{R} = 8.314\ \mathrm{J/(mol \cdot K)}$ is the universal gas constant, and $\mathrm{C_{p,}}_i$ is the specific heat capacity of the mixture in $\mathrm{J/(mol \cdot K)}$. It is written as

$$\mathrm{C_{p,}}_i = \sum_1^j \mathrm{X}_{ij} \mathrm{C_{p,}}_{ij} \tag{8}$$

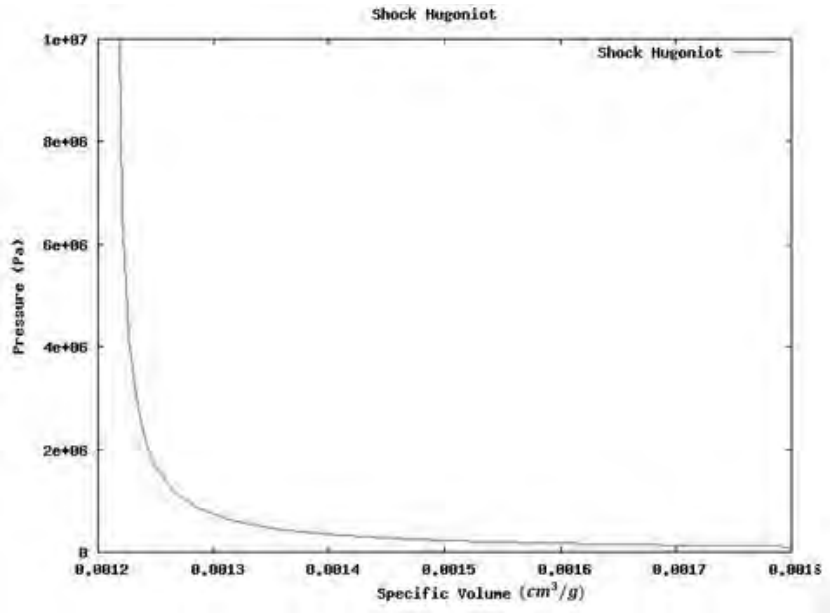

Figure 1: Shock Hugoniot for the Combustion of Acetylene using the Calorically Perfect Gas Equation of State

where the summation runs over the j species for reactants ($i = 0$) and products ($i = 1$); $\mathrm{C_{p,}}_{ij}$ is the specific heat capacity, $\mathrm{C_p}$, in $\mathrm{J/(mol \cdot K)}$ of the j^{th} species; and $\mathrm{X}_{ij} = \rho_{ij}/\rho_i$ is the mass fraction of the j^{th} species, where ρ_{ij} is the partial density of that species. The simple case of the combustion of acetylene, shown below, is considered.

$$\mathrm{C_2H_2} + \frac{5}{2}\mathrm{O_2} \rightarrow 2\mathrm{CO_2} + \mathrm{H_2O} \tag{9}$$

For the combustion of acetylene, a graph of equation (6) produces a shock Hugoniot as seen in Figure 1. With $q_{C_2H_2} = 1255.5\ \mathrm{kJ/mol}$[4], the detonation Hugoniot for this reaction is produced and shown with the shock Hugoniot in Figure 2.

Now that the basic procedure is established, we may develop a Hugoniot for a more sophisticated equation of state. The JWL equation of state may be written as [5]

$$p = A\left(1 - \frac{w}{R_1 V}\right)\exp(-R_1 V) + B\left(1 - \frac{w}{R_2 V}\right)\exp(-R_2 V) + \frac{we}{V} \tag{10}$$

where A, B, w, and $R_{1/2}$ are unique constants specified for each explosive, $V = v_1/v_0$, and e is the volumetric internal energy and is given by $e = \rho_0 E$, where E is specific internal energy. Now the form of equation (5) must include specific internal energy instead of sensible enthalpy

$$E_1 - E_0 - q = \frac{1}{2}(p_1 + p_0)(v_0 - v_1) \tag{11}$$

Solving (10) for E and substituting into (11), we obtain[6]

$$p_1(V) = \frac{\left\{\frac{V}{w}\left[A\left(1-\frac{w}{R_1V}\right)\exp(-R_1V)+B\left(1-\frac{w}{R_2V}\right)\exp(-R_2V)\right]+p_0\left[\frac{1-V}{2}\right]+\frac{q}{v_0}+\frac{E_0}{v_0}\right\}}{\left\{\frac{1}{2}\left[\left(\frac{w+2}{w}\right)V-1\right]\right\}} \tag{12}$$

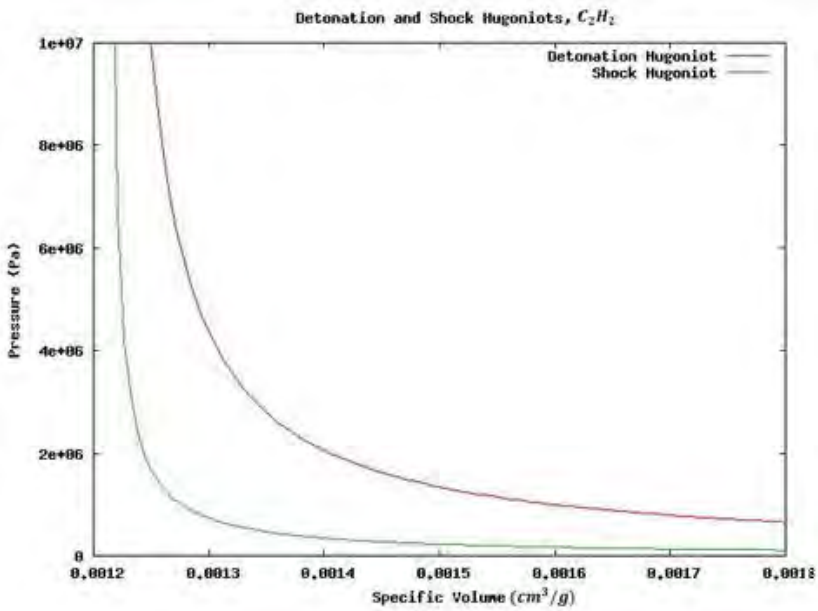

Figure 2: Detonation and Shock Hugoniots for the Combustion of Acetylene using the Calorically Perfect Gas Equation of State

where E_0 represents the internal energy of the solid explosive, and is given by

$$E_0 = \mathrm{C_v T_0} \tag{13}$$

where $\mathrm{T_0}$ is the initial temperature, and $\mathrm{C_v}$ is its constant volume specific heat capacity. Approximate values of $\mathrm{C_v}$ are used for the explosives of interest. Given an initial temperature of about $10^3\mathrm{K}$ and a specific heat capacity for an average explosive of about $10^3\mathrm{J/(kg \cdot K)}$, E_0 is on the order of $10^5\mathrm{J/kg}$. Compared to the other terms in (12), its contribution to pressure is negligible, so E_0 may be set to zero. Figures 3 through 7 show the JWL detonation Hugoniots for Trinitrotoluene (TNT), Cyclo-tetramethylene tetranitramine (HMX), a Cyclo-trimethylene trinitramine or RDX derivative (Composition C-4), a Triaminotrinitrobenzene derivative (PBX-9502) and Pentaerythritol tetranirate (PETN), respectively. The JWL equation of state parameters are provided in Table 1.[7]

Table 1. JWL Equation of State Parameters

Explosive	A (Mbar)	B (Mbar)	R_1	R_2	ω
TNT	3.712	0.3231	4.15	0.95	0.30
HMX	7.783	0.07071	4.20	1.00	0.30
C-4	6.0997	0.1295	4.5	1.4	0.25
PBX-9502	4.603	0.9544	4.0	1.70	0.48
PETN	5.731	0.20160	6.00	1.80	0.28

In the interest of comparison, a products-based shock Hugoniot is shown for each explosive; its locus is obtained by setting $q = 0$ in the product JWL Hugoniot formula (12). In doing so, we can illustrate the shift in the Hugoniot locus caused by the detonation energy term. In practice, solid explosive materials require different equations of state (usually not the JWL equation) in order to capture the correct response to shock pressure. This solid phase equation

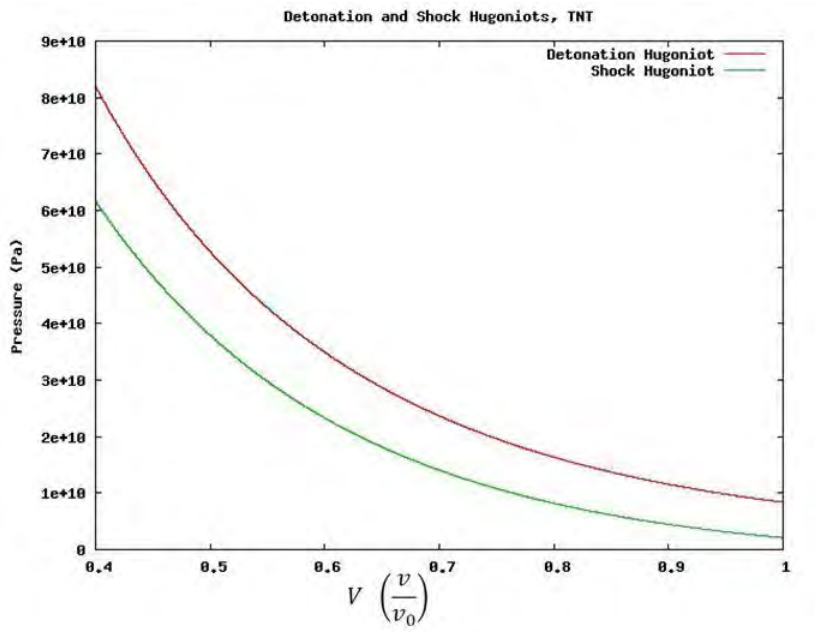

Figure 3: Detonation and Shock Hugoniots for TNT using the JWL Equation of State

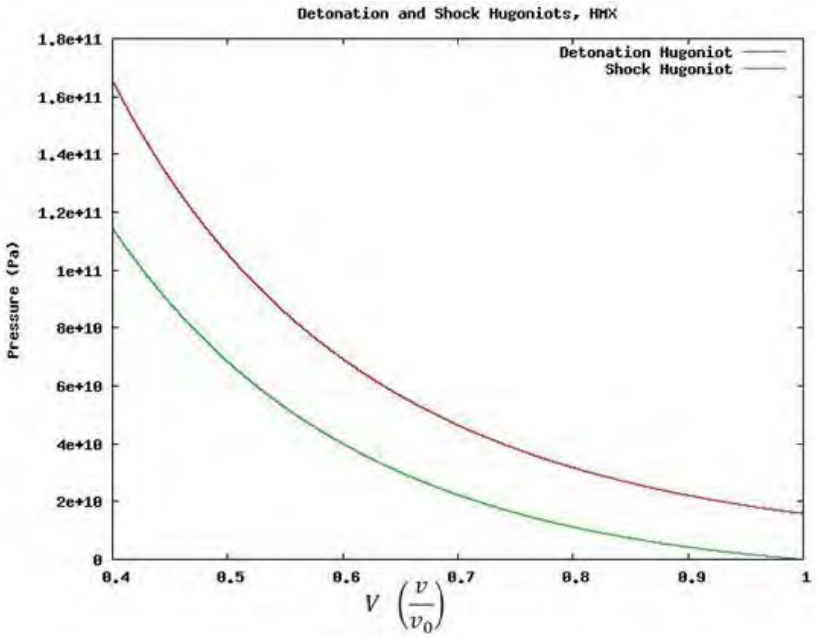

Figure 4: Detonation and Shock Hugoniots for HMX using the JWL Equation of State

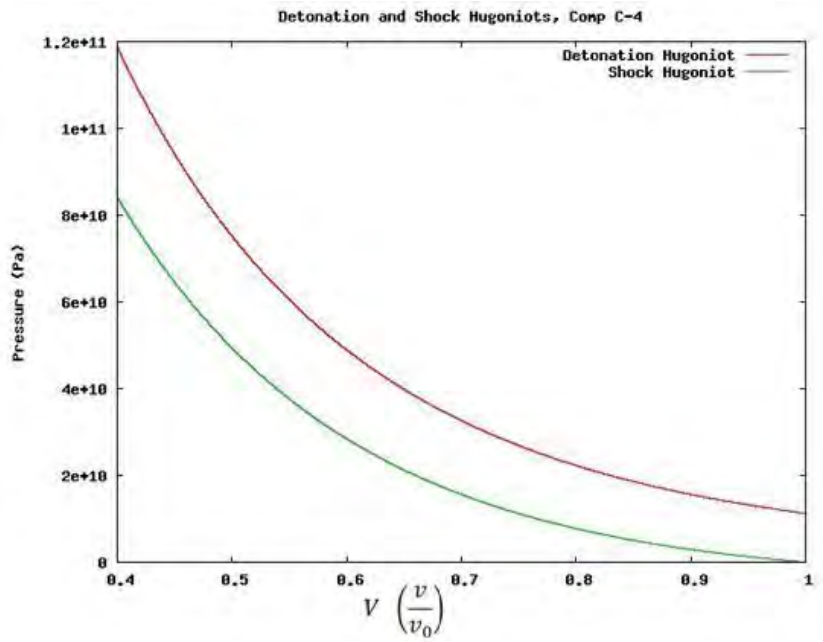

Figure 5: Detonation and Shock Hugoniots for Composition C-4 using the JWL Equation of State

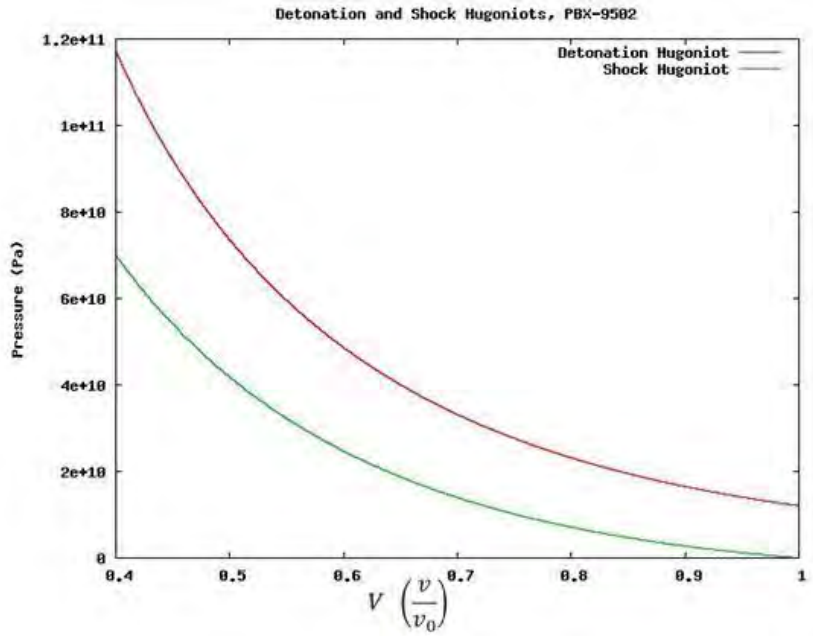

Figure 6: Detonation and Shock Hugoniots for PBX-9502 using the JWL Equation of State

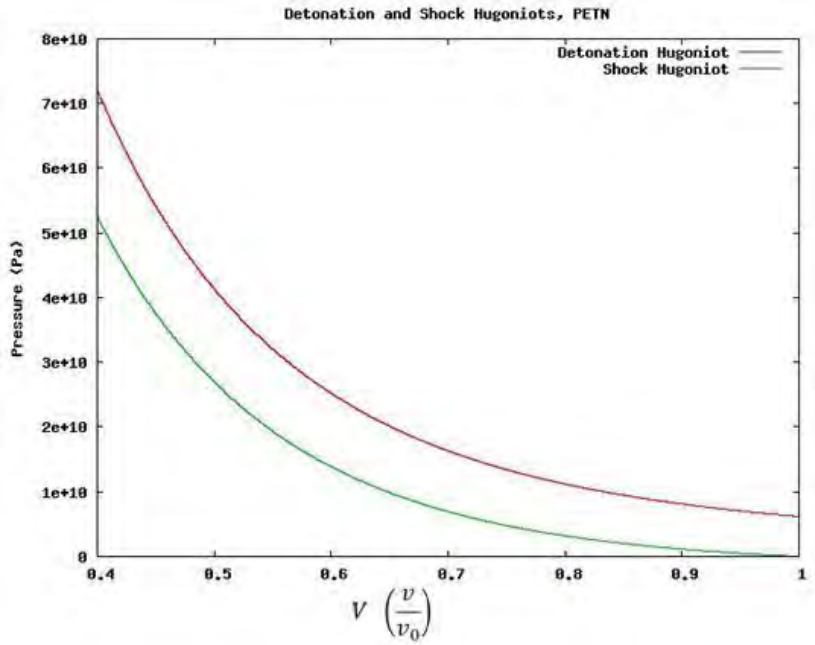

Figure 7: Detonation and Shock Hugoniots for PETN using the JWL Equation of State

(e.g., a Mie-Grüneisen or Hayes formula, suitably calibrated for the explosive) is substituted in (12) with $q = 0$ to obtain the shock Hugoniot for the solid explosive.

With the background provided on the conservation laws and on the equation of state for the detonation products, we may now determine the properties of the flow field at detonation conditions. In the ideal theory, detonation is modeled as an instantaneous phase transition. The solid explosive originally at the state P_0, ρ_0 transitions directly to the steady state detonation conditions with pressure and density, P_1 and ρ_1, respectively. That is to say, the phase transformation does not move along the Rayleigh line in time. The change in properties is effectively discontinuous. Any realizable detonation condition must lie on both the Detonation Hugoniot and the Rayleigh Line as shown in Figure 8. The two solutions shown correspond to strong and weak detonations; however, the strong detonation state is rarely observed. The weak detonation is generally not observed.[1] The most commonly observed detonation condition is Chapman-Jouguet (CJ) detonation. This state exists where the Rayleigh Line is tangent to the Detonation Hugoniot, a position referred to as the CJ Point.[4] It is also the state found in steady detonations. The existence of the CJ point is not deduced from the conservation laws. Rather its existence is explained from a conjecture involving detonation physics substantiated by empirical measurements.[1] This point may be found by plotting a function F, defined as the difference between the Rayleigh line and detonation Hugoniot slopes, and finding its zero. A computer program is used to split up the plot into regions ΔV wide in order to determine at which V the sign of F changes, indicating a root. The function F is determined to be

$$F = \frac{p_1(V) - p_0}{V - 1} - \frac{p_1(V^+) - p_1(V^-)}{\Delta V} \tag{14}$$

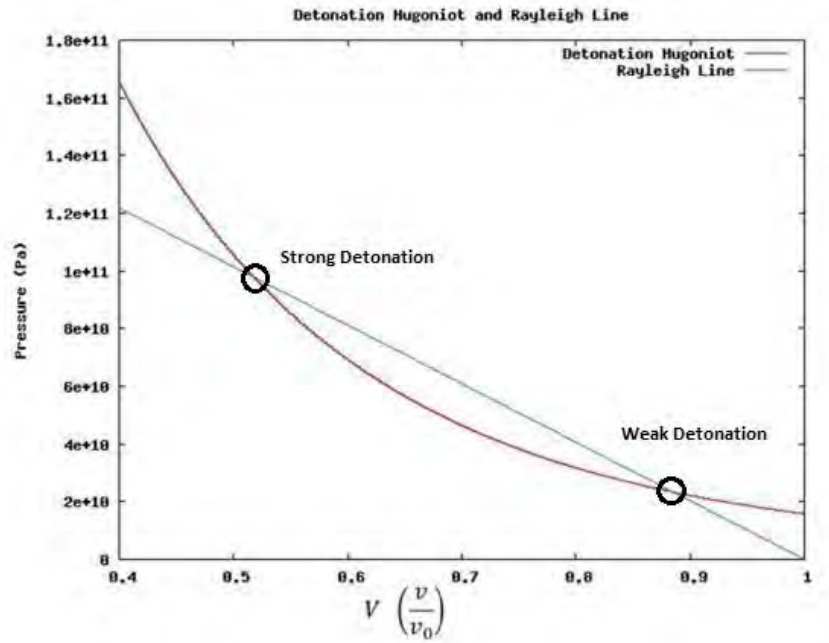

Figure 8: Two Possible Detonation States Identified by Intersection of Rayleigh Line and Detonation Hugoniot

where $p_1(V)$ is given by (12). In equation (14), we have introduced some new notation. Let

$$p_1(V^{\pm}) = p_1(V \pm \tfrac{\Delta V}{2}), \tag{15}$$

where ΔV is given by

$$\Delta V = \tfrac{V_{\max} - V_{\min}}{k} \tag{16}$$

$V_{\max}$ is a reasonable upper bound on the value of V; $V_{\min}$ is a reasonable lower bound on the value of V, and k is the number of sections comprising the region between $V_{\max}$ and $V_{\min}$. The parameter k is assigned a value of 100,000 in order to accurately the value of V_{CJ} where $F(V_{CJ}) = 0$ as in (14). In the next section, this algorithm is employed to calculate the Chapman-Jouguet detonation conditions for a series of explosives.

2.2 Results

The simple root finding algorithm (14-16) developed in the preceding section has been used to determine the CJ conditions for the legacy explosives TNT, HMX, Composition C-4, PBX-9502 and PETN. The CJ points are graphed on the detonation Hugoniots for these materials in Figures 9 through 13, respectively, for the subject explosives. The CJ pressures are validated exhibiting excellent agreement with archival data. This information is provided in Table 2.

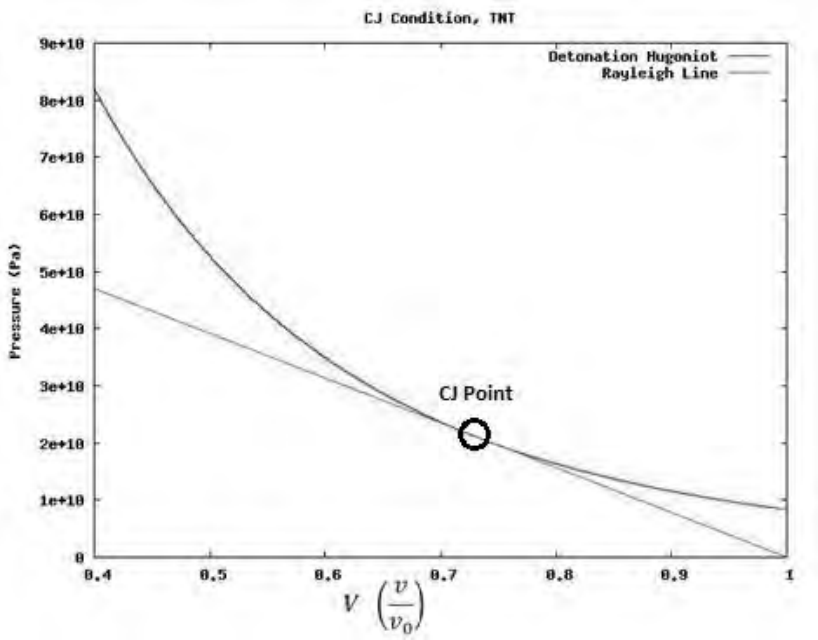

Figure 9: Chapman-Jouguet State for TNT

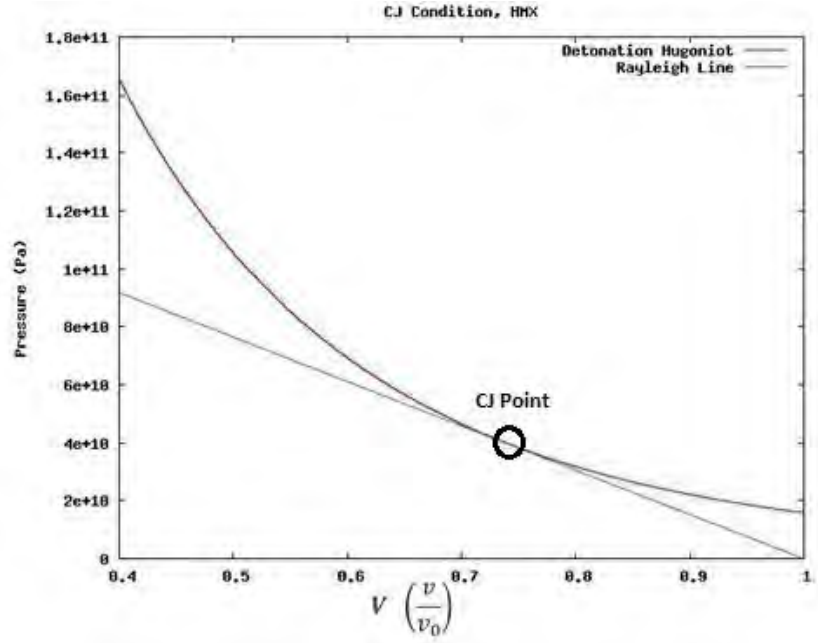

Figure 10: Chapman-Jouguet State for HMX

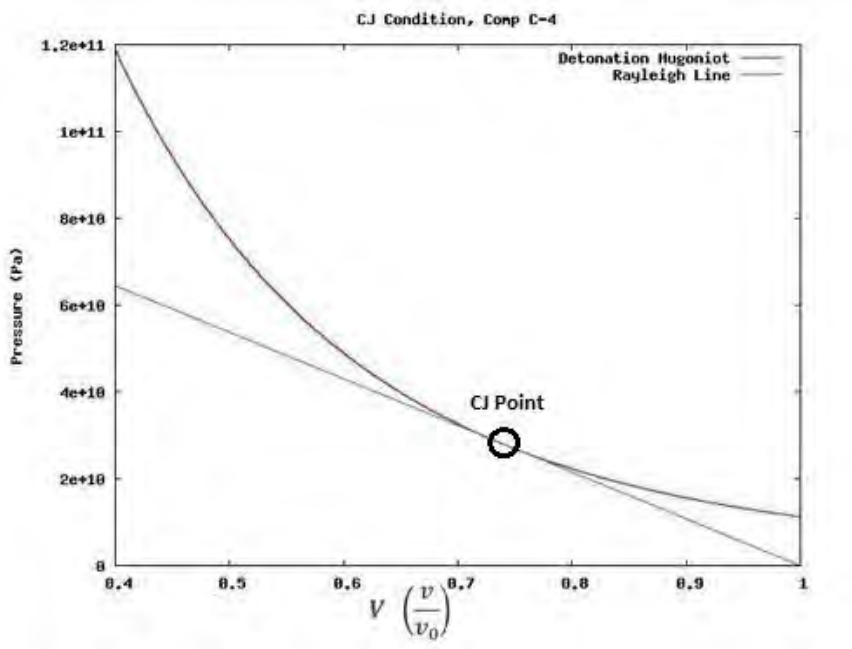

Figure 11: Chapman-Jouguet State for Composition C-4

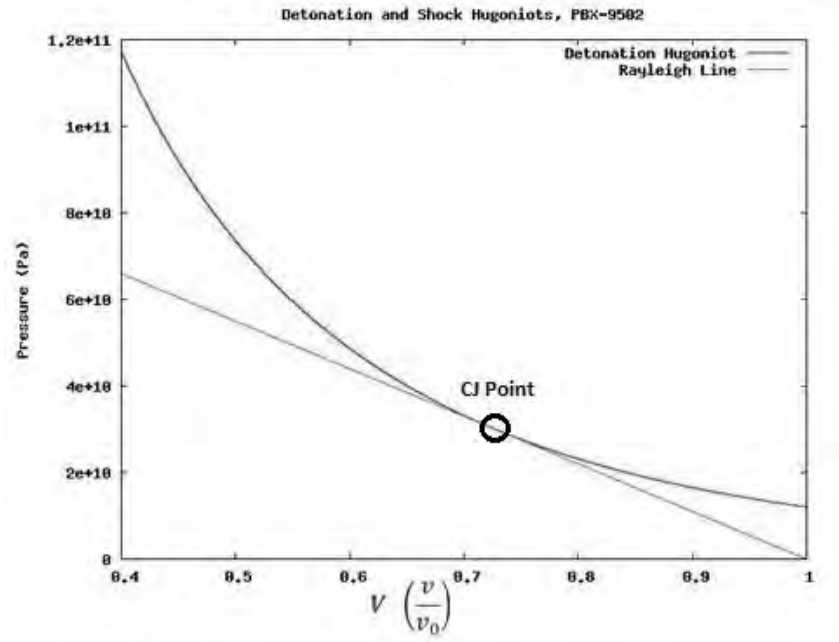

Figure 12: Chapman-Jouguet State for PBX-9502

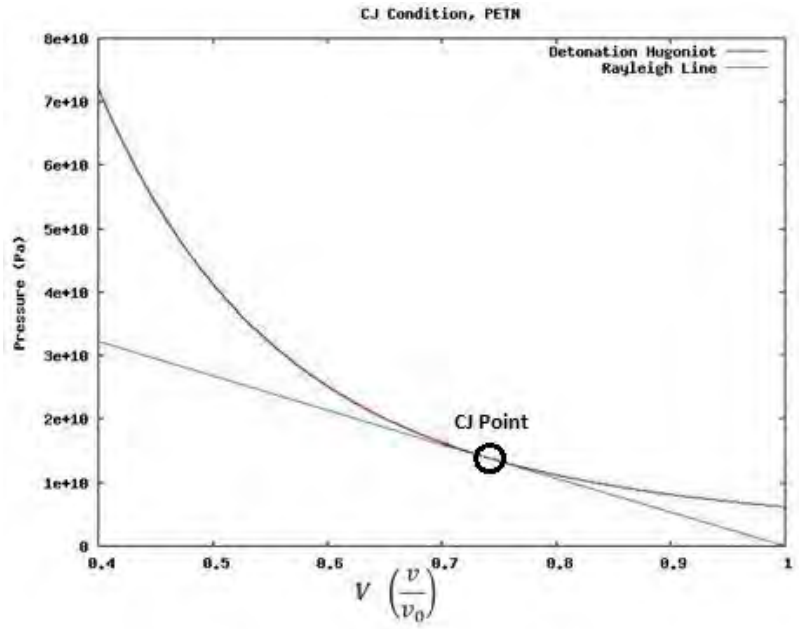

Figure 13: Chapman-Jouguet State for PETN

Table 2. Validation of Numerically Calculated Chapman-Jouguet Pressures

Explosive	CJ Pressure (GPa)	
	Calculated	Reported[7]
TNT	21.0	21.0
HMX	42.2	42.0
Composition C-4	28.0	28.0
PBX-9502	30.2	30.2
PETN	14.0	14.0

It is evident that this algorithm generates CJ pressures matching the known values for the subject explosives within one-half percent error. The largest discrepancy is associated with the CJ pressure for HMX. Our prediction is 42.0 GPa, while the value reported by the previous study is 42.2 GPa.[7] Dobratz reports that the archival CJ pressure for HMX is estimated[7], so the disagreement between this value and the calculated pressure is minor. This study is important because of its fundamental nature and its wide range of applicability. The Hugoniot equation, Rayleigh Line, and CJ conditions all arise naturally from the conservation laws and the JWL equation of state. Although the JWL equation of state remains controversial, it still remains as a workhorse in performing this type of calculation, and it is a natural extension of the ideal theory based upon a single "measurement" of detonation energy (unlike the combustion of acetylene). In the next section, we introduce finite rate blast chemistry where each chemical reaction existing in the blast has its own specification for reaction energy.

3.0 SIMULATING DETONATION SOOT FORMATION

3.1 Technical Approach

The preceding section presents ideal detonation theory from the standpoint of combustion because detonation, like combustion, is a complex chemistry problem. There are two major differences between combustion and detonation. In the first place, the chemical rates for detonation are far more rapid than those for combustion. In fact, at the laboratory scale, detonation reactions appear to be nearly instantaneous. Secondly, combustion processes tend to acquire oxygen from their surrounding environment. Explosives contain an amount of oxidizer sufficient to conduct the detonation. When "burned", both fuels and explosives produce a wide array of products. Even simple fuels like methane have reaction mechanisms involving eight or more species. More complex molecules such as HMX may involve one hundred products or more. These products include both gases and solids. The family of solid products denoted as "soot" has acquired a certain "enigmatic" nature.

Neither the composition of nor the mechanism behind the formation of soot via combustion is well understood. For our purposes, soot is assumed to be purely solid carbon, but its formation seems to rely on the presence of one or more chemical precursors, e.g., acetylene. This study is based on a four step model: nucleation, surface growth, oxidation, and agglomeration.[3] The first two steps govern the mass formation, and the last two deal with the interaction of the soot after formation. The present investigation concerns itself with the mass formation of the soot—the first two steps. All calculations are done for each volume element of the simulation grid (or mesh), so many of the units given below—densities, concentrations, etc.—are for mixture-based quantities.

Some studies suggest that of particular importance to soot growth is the presence of acetylene, C_2H_2, which correlates with a very rapid initial growth phase.[3] In this case, the soot precursor, acetylene, is assumed to arise from Lauryl methacrylate (LMA), a component of the HMX-based explosive. A further assumption made is that some active soot (carbon) nuclei are formed from the breakdown of acetylene [3]

$$C_2H_2 \rightarrow 2C(s) + H_2 \tag{17}$$

The reaction rate, then, is given as[3]

$$R_1 = k_1(T)[C_2H_2] \tag{18}$$

where R_1 is given in $\mathrm{mol/(cm^3 \cdot s)}$, and $[C_2H_2]$ is the current concentration of acetylene in the mixture and is given in mol/cm^3. The rate constant $k_1(T)$, in s^{-1}, is given by[3]

$$k_1(T) = A\exp(E_a / RT) \tag{19}$$

where E_a is the activation energy and R is the gas constant for acetylene. The literature states has $E_a/R = 21{,}100$ K and the pre-exponential factor $A = 10{,}000\ s^{-1}$ for a C_2H_4 (ethylene) flame burning with an oxidant stream of 22% O_2 and 78% N_2.[3] Note that ethylene is a chemical precursor for acetylene. The second step is the adsorption of C_2H_2 on the surface of the soot particles[3], i.e.,

$$C_2H_2 + nC(s) \rightarrow (n+2)C(s) + H_2 \quad (20)$$

An arbitrary soot particle size n is chosen to begin this step of the soot formation process. An initial particle size has been reported as 20 to 50 carbon atoms, so n is chosen as 20.[8] This reaction is again governed by the acetylene concentration, but also by the number of active adsorption sites, which is related to the surface area of the particle. Studies have shown that, on the average, older particles are less reactive than younger particles.[3] To account for this decrease in reactivity with age, the number of reaction sites is assumed to be proportional to the square root of the surface area available locally in the flame. So the governing reaction rate is[3]

$$R_2 = k_2(T) f(S) [C_2H_2] \quad (21)$$

where $[C_2H_2]$ is the current concentration of acetylene in the mixture and is given in mol/cm^3; $f(S)$ is the square root of the available surface area S, and $k_2(T)$ is the rate constant. Based again on the mixture, S is given in units of cm^2/cm^3 and is written as[3]

$$S = \left(d_p^2\right)(\rho N) \quad (22)$$

where ρ, in g/cm^3, is the mixture density. Also, N is the total number of soot particles per gram of mixture, and d_p is the diameter of each soot particle, given as[3]

$$d_p = \left(\frac{6}{\pi}\frac{1}{\rho_c}\frac{Y_{C(s)}}{N}\right)^{\frac{1}{3}} \quad (23)$$

Note that $\rho_c = 2\ \mathrm{g/cm^3}$ is the soot density (based upon a reasonable value for the density of carbon[3]), and $Y_{C(s)}$ is the mass fraction of solid carbon in the mixture. To create a more realistic soot model, it is desirable to build a number density evolution equation into LESLIE3D as a part of its governing equations. This equation actually captures the evolution of the number of soot particles per unit volume in time and space. Implementing this method requires further development of LESLIE3D and is reserved for future research. At present, we assume that N is fixed at 100 particles/g of mixture. The mass fraction is given by[3]

$$Y_{C(s)} = \frac{[C(s)]M_{C(s)}}{\rho} \quad (24)$$

where $[C(s)]$ is the concentration of solid carbon in mol/cm^3, and $M_{C(s)}$ is the molar mass of solid carbon, $12.011\ \mathrm{g/mol}$. From equations (22-24), equation (21) becomes[3]

$$R_2 = k_2(T)[C_2H_2]\left(\pi\right)^{\frac{1}{2}}\left(\frac{6M_{C(s)}}{\rho_c}[C(s)]\right)^{\frac{1}{3}}(\rho N)^{\frac{1}{6}} \quad (25)$$

where the rate constant $k_2(T)$, in cm$^{3/2}$/cm/s for the soot , is given by[3]

$$k_2(T) = A\exp(-E_a / RT) \quad (26)$$

where $E_a/R = 12{,}100$ K and the preexponential factor $A = 6{,}000$ cm^3/cm/s has been determined for a C_2H_4 flame burning with an oxidant stream of 22% O_2 and 78% N_2.[3] Two other reactions, the combustion of carbon monoxide[9] and the combustion of hydrogen[10], which do not directly produce soot are included in this model, i.e.,

$$2CO + O_2 \rightarrow 2CO_2 \quad (27)$$

$$2H_2 + O_2 \rightarrow 2H_2O \quad (28)$$

For these reactions, the pre-exponential factors (A) are $3.98 \times 10^{14}\ s^{-1}$ and $1.8 \times 10^{13}\ s^{-1}$. E_a / R is set equal to 20,130 K and 17,614 K, respectively.[9,10] The entire mechanism used for this model may be written as

$$C_2H_2 \rightarrow 2C(s) + H_2 \quad (28)$$

$$C_2H_2 + nC(s) \rightarrow (n+2)C(s) + H_2 \quad (29)$$

$$2CO + O_2 \rightarrow 2CO_2 \quad (30)$$

$$2H_2 + O_2 \rightarrow 2H_2O \quad (31)$$

with reaction rate information given in Table 3. [3,9,10]

Table 3. Reaction Rate Information

Reaction	A	E_a/R (K)
Soot Nucleation	10,000 s^{-1}	21,100
Soot Surface Growth	6,000 $cm^{3/2}/cm/s$	12,100
CO Combustion	3.98×10^{14} s^{-1}	20,130
H_2 Combustion	1.8×10^{13} s^{-1}	17,614

A subroutine representing this reaction mechanism has been written in standard CHEMKIN CKWYP form and integrated into LESLIE3D.[11] LESLIE3D calls the CKWYP subroutine and solves for the species concentrations using its locally dynamic subgrid kinetic energy model.[12] The filtered governing equations (including the species equations) are closed with the use of the Eddy Break-Up turbulent chemical reaction closure model.[13] This model ensures that the reaction rates are properly limited for turbulent mixing. Without this type of closure, the kinetic reaction rates are over-predicted. The following section of the report contains the results of this model applied to a typical explosive.

3.2 Results

The reaction mechanism described in Section 3.1 has been applied to the blast field produced by the detonation of an HMX-based explosive. Although LESLIE3D cannot accomplish the actual detonation, the detonation is conducted in a separate computer code and imported into LESLIE3D. LESLIE3D's simulation begins at 8.5 μs of problem time. We compare the results obtained for the pure nucleation model with those of the latest model that includes nucleation with the surface growth reaction step. Figure 14 shows the total number of carbon atoms in the simulation with respect to time for pure nucleation, while Figure 15 shows

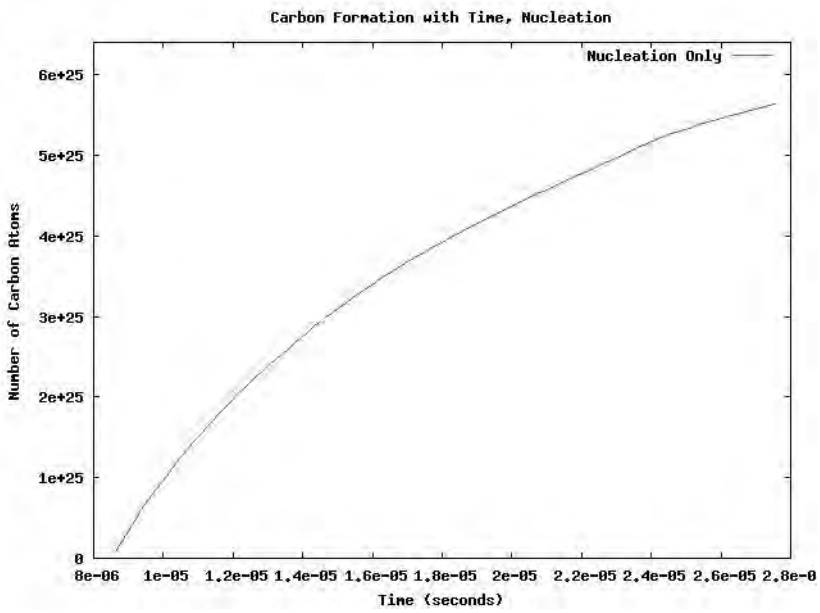

Figure 14: Soot Production via Pure Nucleation for an HMX-based Explosive

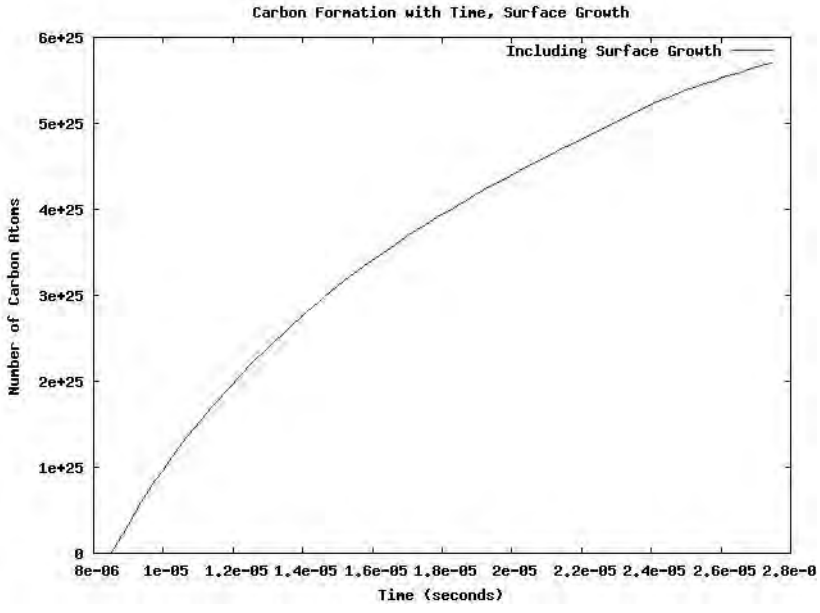

Figure 15: Soot Production via Nucleation Plus Surface Growth for an HMX-based Explosive

the total number of carbon atoms in the simulation with respect to time for the inclusion of terms representing surface growth through adsorption. As we may expect from an examination of the reaction mechanism, the soot nucleation process is quite strong in the early moments of the blast. (Note that this model contains no soot destruction mechanism). Yet the slopes of the curves in Figures 14 and 15 begin to reduce at about 15 μs. This effect is likely due to the relatively small amount of acetylene used to initialize the simulation. Recall that our original acetylene concentration is based upon an assumed set of decomposition products for Lauryl methacrylate, a

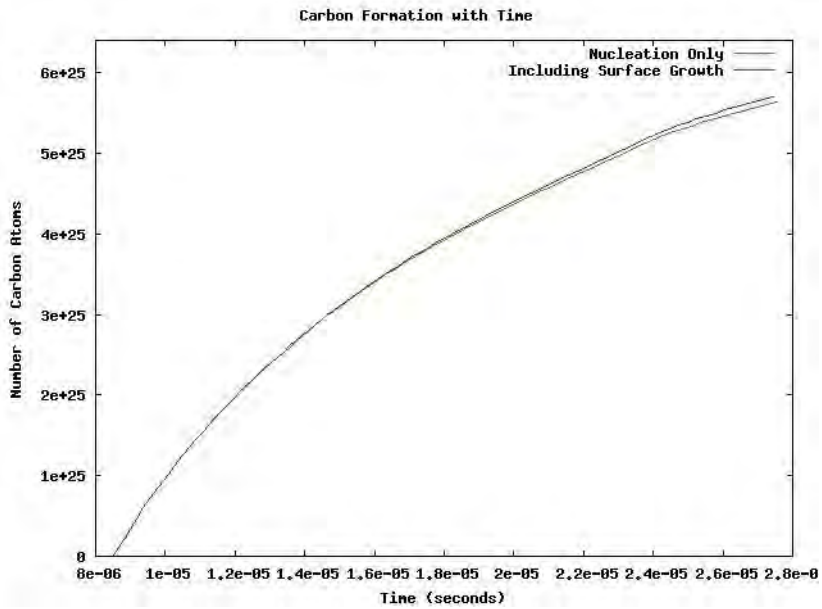

Figure 16: A Comparison of Soot Production via Nucleation and Nucleation Plus Surface Growth for an HMX-based Explosive

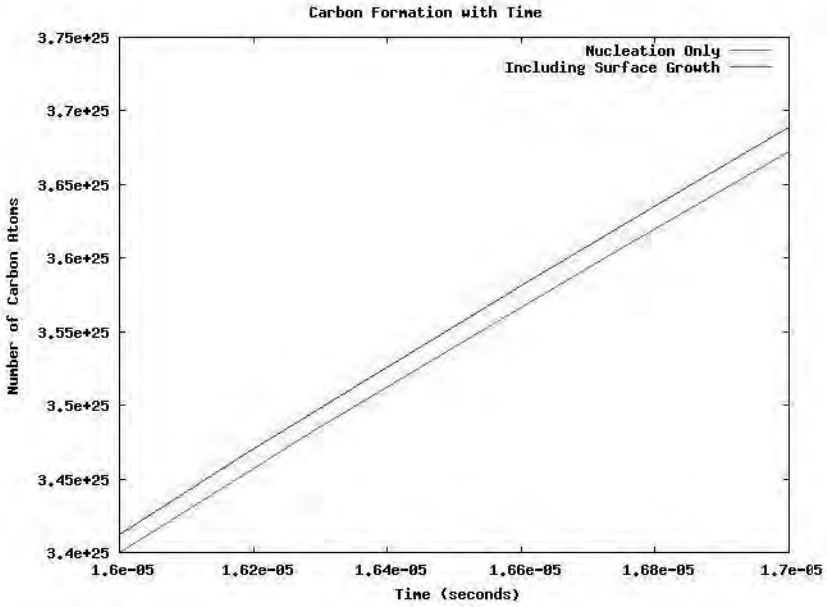

Figure 17: A Comparison of Soot Production via Nucleation and Nucleation Plus Surface Growth for an HMX-based Explosive over the Time Period of 16 µs to 17 µs

constituent of the explosive. Figure 16 shows both plots for pure nucleation and surface growth in order to facilitate direct comparison. The difference between these two curves is small, but the surface growth term does increase soot production, especially at later times. By magnifying the plot, may obtain a clearer view of the differences. Figure 17 shows a magnified view of soot production from 16 to 17 µs while Figure 17 shows soot production over the time period of 25 to 27.5 µs. At 16.5 µs, the difference (for the entire blast field) is approximately 2.4 g of carbon. However, the increase in surface growth causes the production of carbon to escalate to about 14 g at 26.5 µs. Bearing the number of assumptions in mind, it is interesting to see the quantitative

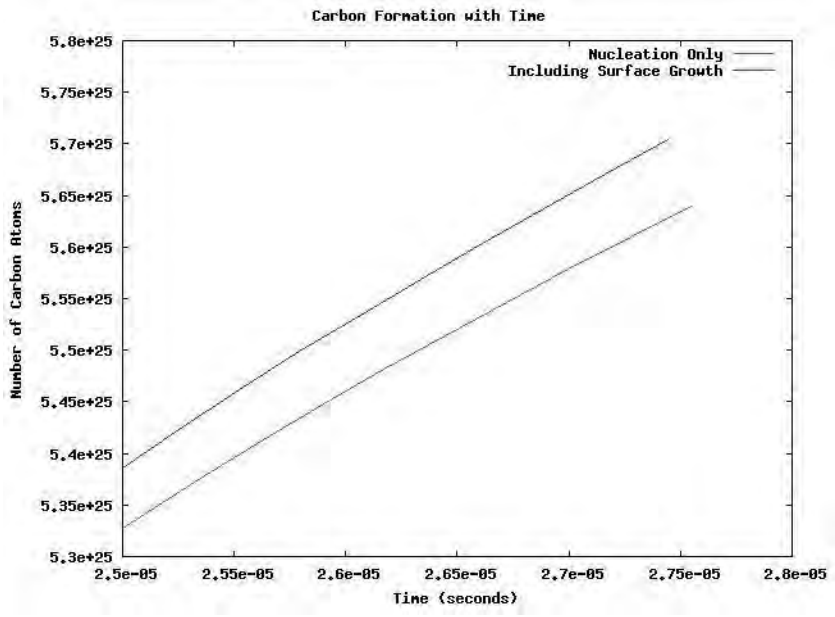

Figure 18: A Comparison of Soot Production via Nucleation and Nucleation Plus Surface Growth for an HMX-based Explosive over the Time Period of 25 μs to 27.5 μs

differences in soot production predicted by this simple model. In a follow-on step, it would be instructive to see the effects of including soot oxidation within the reaction mechanism. This process is relatively easy to integrate into the overall reaction mechanism. Yet, it is perhaps of greater importance to first improve the selection of detonation products. The present set of detonation products is too simple. Many possible byproducts of HMX's detonation are overlooked. The presence of more products may significantly alter blast chemistry.

4.0 CONCLUSIONS AND RECOMMENDATIONS

The present work takes some preliminary steps in considering the processes of detonation and the subsequent burn of detonation products in the blast field in a unified way. Detonation has most often been treated from the standpoint of shock physics. The detonation wave is often considered to be a discontinuity propagating through the explosive. We have implemented this theory and have shown that it produces good results for pressure. Yet, it is important to realize that detonation is a chemical reaction that takes place over a very small region of space. This reaction creates products, chemical species that react with the surroundings. Moreover, these reactions create solid carbonaceous products collectively called "soot". The second part of this study considers a proposed mechanism for the production of soot in the blast field for an HMX-based explosive. This mechanism is tested using the LESLIE3D multiphase physics computer code. Using turbulent chemistry, LESLIE3D produces time accurate curves for soot production starting from an initial detonation solution. The model gives good qualitative results—more soot is being produced when the surface growth step is included, and we observe a proper limiting of carbon production as the initial carbon field begins to disperse and rarefy. The difference in the actual number of particles between the two models seems relatively small, but does result in an appreciable increase in soot mass. Remember that even in regular combustion processes, soot production is often low. It is often detected as powdery smears on engine exhaust piping. It is also apparent that fixing the total number of soot particles at 100 makes for a low estimate, as the actual number of particles is on the order of 10^{25} for most of the simulation. Moreover, we know that, in reality, this number actually changes. Representing this aspect of the physics requires a better soot model incorporating an evolution equation for the soot particle number density. One could also expand the overall reaction mechanism for detonation products to include soot oxidation, soot agglomeration, and governing reactions for other by-products of the HMX-based explosive. One could represent soot transport by including massive Lagrangian particles. These particles can propagate through the flow field under inertial and drag forces. This aspect of the model may provide better ideas of soot dispersion. That is to say, soot that disperses more quickly cools more rapidly. It is also prudent to study the overall extraction of energy release data throughout the blast field to obtain greater insight into the effect of these reactions on the overall blast chemistry. The best recommendation for the enhancement of this research is that these numerical simulations continue in parallel with an experimental investigation into both the gaseous detonation products as well as into identification of the soot's chemical make-up created by explosives of choice.

REFERENCES

1. Lee, J.H.S., **The Detonation Phenomenon**, Cambridge University Press, 32 Avenue of the Americas, New York, NY, 2008, pp. 26-33

2. Erlebacher, G., Hussaini, M.Y., Speziale, C.G. and Zang, T.A., "Toward the large-eddy simulation of compressible turbulent flows", *Journal of Fluid Mechanics*, **238**, 1992, pp. 155-185

3. Leung, K.M., Lindstedt, R.P., and Jones, W.P., "A Simplified Reaction Mechanism for Soot Formation in Nonpremixed Flames", *Combustion and Flame*, **87**, 1991, pp. 289-305

4. Glassman, I., **Combustion, 3rd Ed.**, Academic Press, 525 B Street, Suite 1900, San Diego, California 92101-4495, USA, 1996, pp. 512, 513, 519

5. Davis, W.C., "Shock Waves; Rarefaction Waves; Equations of State", Zukas, J.A., Walters, W.P., **Explosive Effects and Applications**, Springer-Verlag, New York, 2003

6. Nance, D.V., Lecture, Air Force Research Laboratory Summer Internship Program, Eglin Air Force Base, Florida, 6 June 2011

7. Lawrence Livermore National Lab, **LLNL Explosives Handbook. Properties of Chemical Explosives and Explosive Simulants.** Dobratz, B.M. and Crawford, P.C., Livermore, CA, Jan 1985, pp.8-22,23

8. Greiner, N.R., *Diamonds in the Chemical Products of Detonation*, LA-UR-88-3902, Los Alamos National Laboratory, Los Alamos, New Mexico, 1988

9. Westbrook, C.K. and Dryer, F.L., "Simplified Reaction Mechanisms for the Oxidation of Hydrocarbon Fuels in Flames", *Combustion Science and Technology*, **27**, 1981, pp. 31-43

10. Marinov, N.M., Westbrook, C.K. and Pitz, W.J., "Detailed and Global Chemical Kinetic Model for Hydrogen", **Transport Phenomena in Combustion, Vol. 1**, Taylor and Francis, Washington DC, 1996

11. Kee, R.J., Rupley, F.M., Meeks, E. and Miller, J.A., *CHEMKIN-III: A FORTRAN Chemical Kinetics Package for the Analysis of Gas-Phase Chemical and Plasma Kinetics*, SAND96-8216, Sandia National Laboratories, Albuquerque, NM, May 1996

12. Sankaran, V. and Menon, S., "LES of spray combustion in swirling flows", *Journal of Turbulence*, **3**, No. 2, 2002

13. Fureby, C. and Löfström, C., "Large-eddy simulation of bluff body stabilized flames", *Twenty-fifth Symposium (International) on Combustion, The Combustion Institute*, pp. 1257-1264, 1994.

DISTRIBUTION LIST
AFRL-RW-EG-TR-2011-128

Defense Technical Information Center — 1 Electronic Copy (1 file, 1 format)
Attn: Acquisition (OCA)
8725 John J. Kingman Road, Ste 0944
Ft Belvoir, VA 22060-6218

EGLIN AFB OFFICES:

AFRL/RWOC (STINFO Tech Library Copy) — 1 Copy
AFRL/RW CA-N — Notice of publication only

AFRL/RWG - 1 Copy
AFRL/RWM - 1 Copy
AFRL/RWA - 1 Copy